論文 / 著書情報
Article / Book Information

論題(和文)	
Title(English)	FEM Validation of the Displacement Limitation Effect of Gap Brace
著者(和文)	Luo Chengrui, 佐藤大樹, 笠井和彦, 佐分利和宏, 前田達彦, 増田寛之, OSABEL Dave M
Authors(English)	Chengrui LUO, Daiki SATO, Kazuhiko KASAI, Kazuhiro SABURI, Tatsuhiko MAEDA, Hiroyuki MASUDA, Dave M. OSABEL
出典 / Citation	日本建築学会関東支部研究報告集, Ⅰ, , pp. 293-296
Citation(English)	, Ⅰ, , pp. 293-296
発行日 / Pub. date	2024, 3
権利情報	一般社団法人 日本建築学会

2023年度日本建築学会
関東支部研究報告集 I
2024年3月

FEM Validation of the Displacement Limitation Effect of Gap Brace

構造ー鉄骨構造

正会員 Luo Chengrui[*1] 正会員 佐藤大樹[*2]
〃 笠井和彦[*3] 〃 佐分利和宏[*4]
〃 前田達彦[*4] 〃 増田寛之[*4]
〃 OSABEL Dave M. [*5]

Catastrophic earthquake defense; Gap Brace; Steel frame;
Finite element simulation; Displacement limitation;

1. Introduction

To enhance the structural ductility performance of existing buildings and cope with potential catastrophic earthquakes, a novel seismic device called Gap Brace was proposed collaboratively by Tokyo Institute of Technology (Sato and Kasai Laboratories) and Takenaka Corporation[1)-4)]. The primary objective of the Gap Brace is to restrict the displacement of frame structures during major seismic events, ensuring that the structure does not undergo rapid failure. This allows other energy dissipation devices have sufficient time to absorb and dissipate seismic energy.

The concept design and mechanism of the Gap Brace was first proposed in 2020[1)], showing that it can effectively limit displacement and reduce the required number of dampers in seismic design. In the same year, small-scale test specimens were designed and manufactured for static cyclic load experiment. Tests confirmed that the Gap Brace can enhance the interlayer lateral stiffness only under large force[1)-3)]. Further processing of test results was done in 2022 to investigate frame force distribution and transmission[4)].

While experiment provides real-world behavior of the Gap Brace, interpretation of results is highly dependent on the number of sensors (e.g., strain gages) installed. Whereas, a duly-validated finite element (FE) model of Gap Brace can provide a more information. Hence, this paper carries out three-dimensional FE analysis of the Gap Brace using ABAQUS. Serving as preliminary study, this paper validates the FE modeling by looking into the displacement limitation effect of the Gap Brace.

2. Design concept and scale experiment

2.1 Design concept

As shown in Figure 1, the Gap Brace is designed to remain inactive during minimal interlayer deformation, and actives and limits the displacement of frame during major earthquake. As the story drift in X direction Δx intensifies, surpassing a predefined gap value Δu, the Gap Brace comes into operation. It deforms along with the frame, thereby increasing the lateral stiffness of the frame and reducing the displacement.

Figure 2 provides the visual representation of this ideal mechanism. Here, the shear force of the whole system Fs can be written as:

$$F_s = \begin{cases} K_f \Delta x & , \Delta x \le \Delta u \\ K_f \Delta x + K_b(\Delta x - \Delta u), & \Delta x > \Delta u \end{cases} \quad (1)$$

where K_f denotes the lateral stiffness provided by the frame only; K_b denotes the lateral stiffness provided by the Gap Brace.

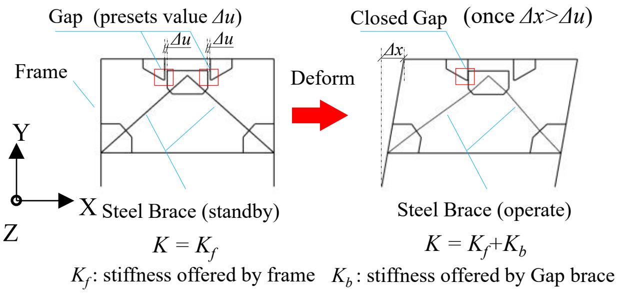

Figure 1 Conceptual Design Diagram

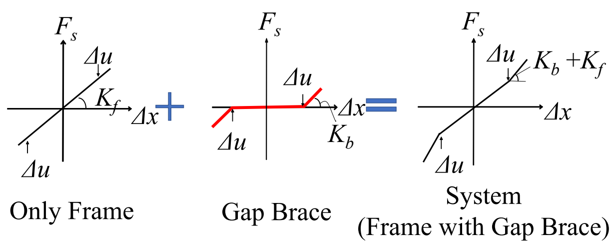

Figure 2 Force – Deformation Relationship

2.2 Small-scale experiment

2.2.1 The small-scale test specimen

FEM Validation of the Displacement Limitation Effect of Gap Brace

Chengrui LUO, Daiki SATO, Kazuhiko KASAI,
Kazuhiro SABURI, Tatsuhiko MAEDA,
Hiroyuki MASUDA, Dave M. OSABEL

Figures 3 and 4 show the schematic diagram and the actual test specimen on the Gap Brace, respectively. As test specimen was a small scale representation of a real-world system (scale ratio = 1:4), the height and width of the test specimen were set to 962.5 mm and 1800 mm, respectively. The materials specifications for each component are indicated in Table 1. The columns cross-section employed 150×150×12 square steel tube, the upper beam cross-section employed 194×150×6×9 H-shaped steel, and the cross-section of the lower beam was set as BH200×100×9×22 H-shaped. Furthermore, four cover plates were bonded to the lower beam to make the lower beam keep elastic.

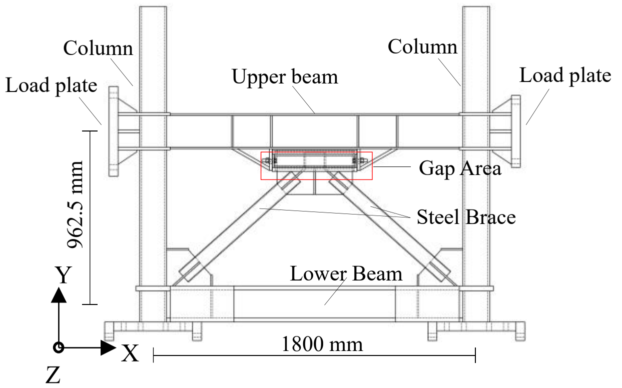

Figure 3 Schematic diagram of Gap Brace

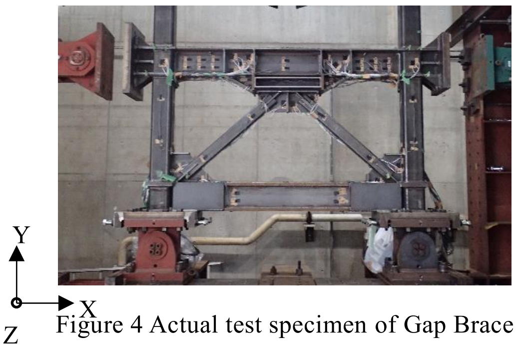

Figure 4 Actual test specimen of Gap Brace

Table 1 the used material for experimental components[2)]

Material	Thickness(mm)	Components
SS400	6 and 9	Upper beam
SN490	9 and 16	Beam hedge, brace head, brace support, lower beam and other components
STKR490	12	Columns
STKR400	3.2	Brace B60 specimen
	4.5	Brace B80 specimen
	12	Columns

Two different specimens of Gap Brace were tested, i.e., one using square tubular steel tube 60×60×3.2 (herein: B60 specimen) and another using 80×80×4.5 (herein: B80 specimen). These two specimens would exhibit different performance during the experiment: the B60 specimen would be significantly damaged, while B80 specimen would remain intact. For both specimens, the prescribed gap value Δu was set at 7.5 mm[4)].

2.2.2 The static loading protocol

The static loading protocol is shown in Figure 5. When the positive load was applied, the left jack (or actuator) was controlled to compress the load plate, and the right jack was maintained in the free state; when the negative load was applied, the opposite was performed. The load force Q_{Jl} and Q_{Jr} of the left and right jacks, respectively, were measured by the inner sensor. The total jack load force Q_J was regarded as a sum of Q_{Jl} and Q_{Jr}. The target load was Q_J = ±400 kN, ±600 kN, ±800 kN, ±1000 kN. Among them, the case of ±1000 kN was cycled twice. By this way, both the performance of the experimental specimens and the displacement limitation effect of the Gap Brace could be studied. In addition, verifying the brace not operate in weak load force case (before Q_J = ±600 kN) was also achieved.

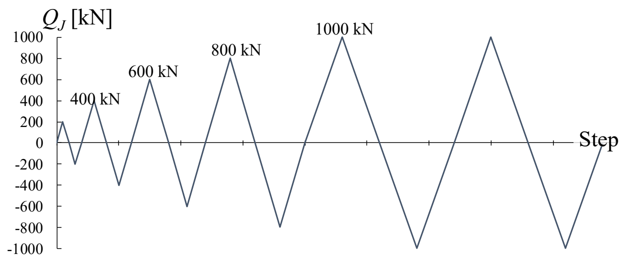

Figure 5 Static-loading protocol

3. Finite Element Model

3.1 Material property of the different

To ensure that the simulation result is close to the experimental result, material experimental data is used for the characteristics of finite element model. Due to the deformation, the nominal stress and nominal strain are needed to transformed into real stress and real strain. For material types SS400 and SN490, linear model in the elastic stage was adopted (e.g., Figure 6 for SS400). Meanwhile, for material types STKR490 and STKR400, multi-stage line model in elastic stage was adopted since they show significant nonlinear characteristics (Figure 7).

3.2 Finite element modelling of test specimens

Figure 8 shows the three-dimensional finite element model of the small-scale test specimens (Figures 3 and 4), implemented in ABAQUS. To make numerical calculations accurate and efficient, important elements (upper beam, columns, and Gap Brace) adopt 20-node integrated elements (C3D20) and others adopt 8-node integrated elements

(C3D8). There are 58,153 elements and 215,170 nodes in total. The reduced integrated element is not adopted, which may lead to the calculation results of the steel structure is not accuracy. In addition, the interactions of the possible collision surfaces in the Gap Brace core area are set as “Hard contact” interface property.

As shown in Figure 9, the base support is considered as fixed boundary conditions, and the load plate is loaded uniformly to simulate the load exerted by the jacks. Moreover, the out of plane direction (Z direction) is set as free in FEM while this direction is constrained in scale experiment, because the FEM doesn’t display significant displacement or deformation in the Z direction.

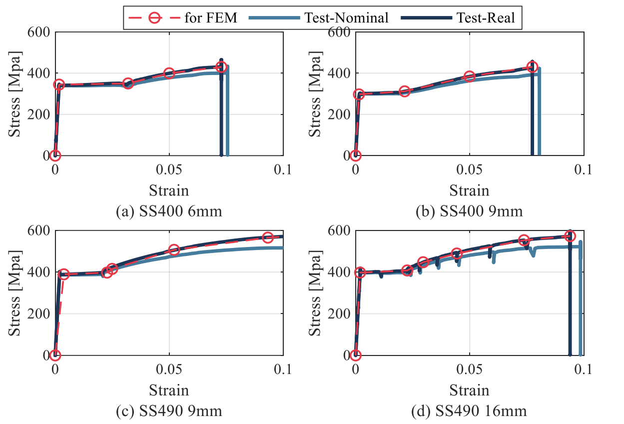

Figure 6 Material property of SS

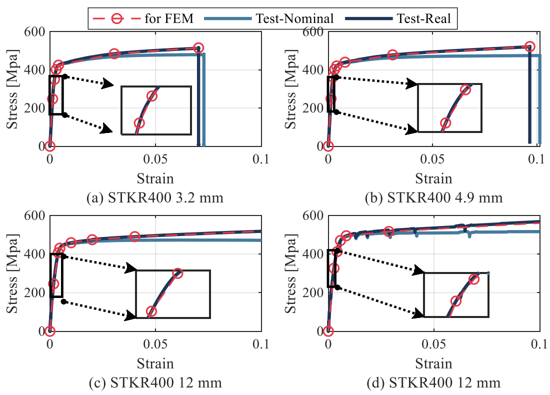

Figure 7 Material property of STKR

4. Result comparison

The simulation results and comparison of the displacement limiting effect for B60 and B80 specimens are shown in Figure 10 and Figure 11, respectively. In these figures, R denotes the story drift ratio, Q_c denotes the columns shear force, Q_b denotes the braces shear force, and $Q_s = Q_c + Q_b$, which are corresponding to Figure 2. The figures show that the experimental and simulated results are very close to each other, indicating that the experiments achieve the expected results and ideal mechanism. In addition, for the B60 specimen, brace deformation failure at 1000 kN was obtained, as shown in Figure 10(d). Due to the significant deformation of the brace, ABAQUS stopped the finite element calculations and therefore further failure modes have not been verified.

To quantify the amount of stiffness enhancement by the Gap Brace activation, linear regression fitting of FEM results using least squares method (LSM) is conducted based on the concept introduced in Figure 2. The Q_s-R plots for B60 and B80 are shown in Figure 12 and 13, respectively. The stiffness of the system clearly improves once the Gap Brace activated. As Table 2 indicates, the lateral stiffness of B60 and B80 increases from 45.13 to 132.87 kN/mm and 46.82 to 162.44 kN/mm, i.e., 2.95 and 3.47 times, respectively. Note that the system stiffness is less than the sum of the frame and brace. This is because the frame had already yielded and the stiffness had decreased.

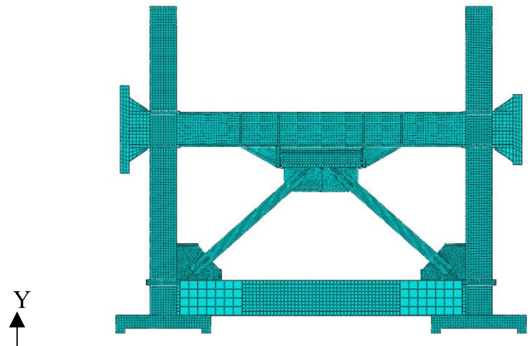

Z

Figure 8 Meshed Finite Element Model

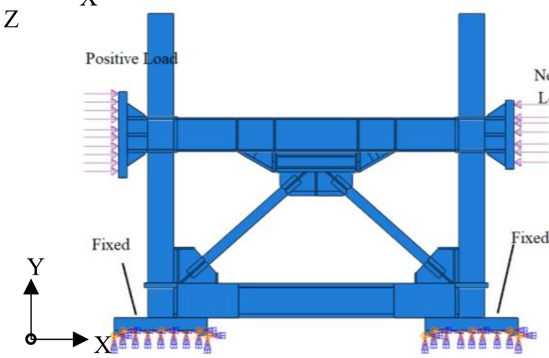

Z

Figure 9 Boundary conditions and load

Table 2 Lateral stiffness (ABAQUS)

Specimen	Components	Stiffness (kN/mm)
B60	Frame only	45.13
	Brace	93.09
	System	132.87
B80	Frame only	46.82
	Brace	135.11
	System	162.44

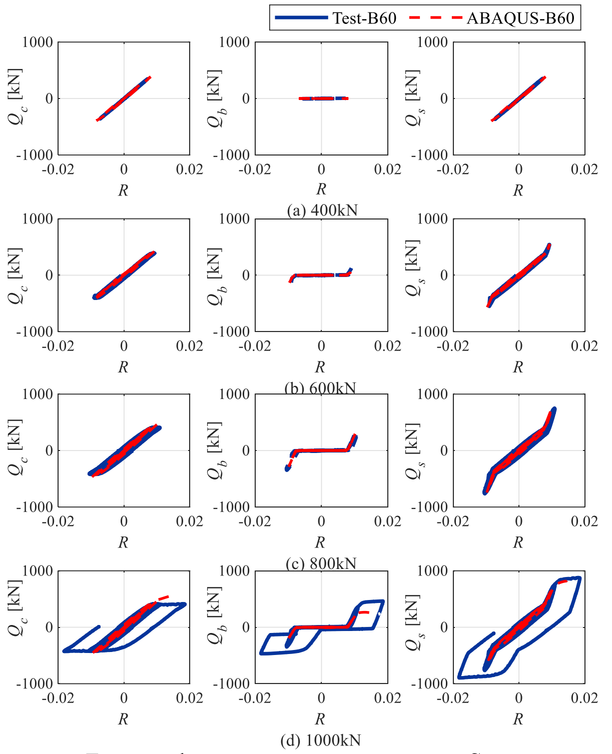

Figure 10 Result comparison of B60 specimen

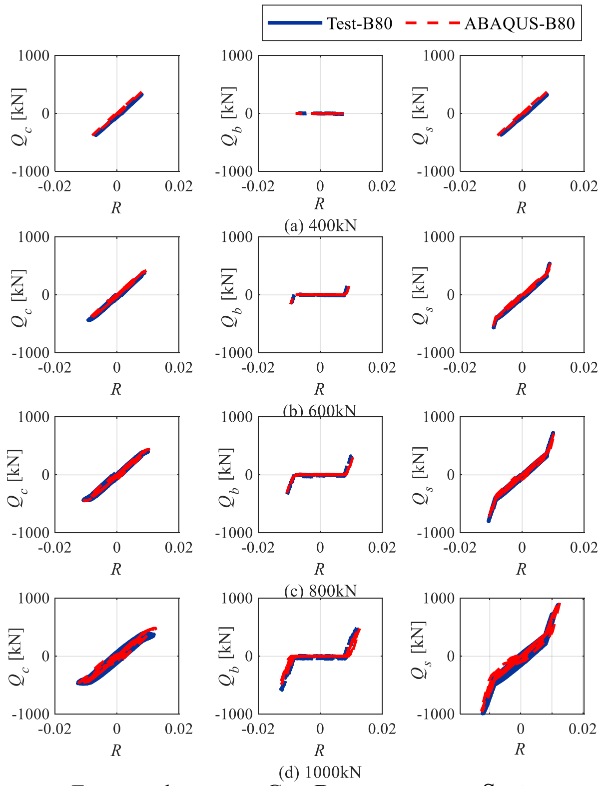

Figure 11 Result comparison of B80 specimen

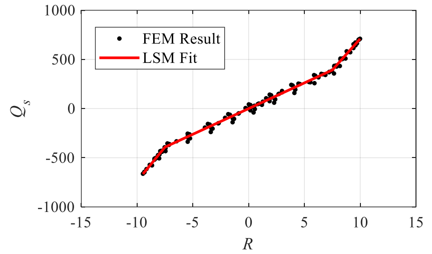

Figure 12 B60 Stiffness fitting by LSM

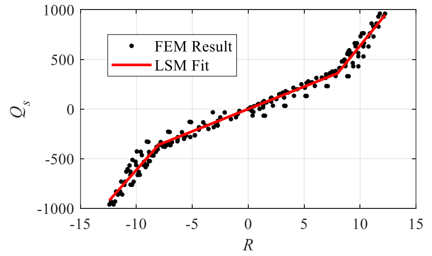

Figure 13 B80 Stiffness fitting by LSM

5. Conclusion

In this paper, the scale static cyclic loading experiment is simulated by software ABAQUS, including test specimens, material properties, boundary conditions and cyclic loads. The result shows that, the finite element model can well simulate the experiment, which is confirmed by the result comparison of the displacement limitation effect of the Gap Brace.

参考文献

1) 上野史也，渡井一樹，佐藤大樹，笠井和彦，佐分利和宏，前田達彦，増田寛之：オイルダンパーと変形制御機構を併用した大振幅地震動に対する既存超高層建物の制振改修設計法，構造工学論文集，pp.353-365, 2020.3.

2) 美濃地正樹，佐藤大樹，笠井和彦，上野史也，渡井一樹，佐分利和宏，増田寛之，前田達彦：ギャップブレースを取り付けた架構の静的載荷実験における事前解析，日本建築学会関東支部研究報告集，pp.477-480, 2020.3.

3) 美濃地正樹，佐藤大樹，笠井和彦，佐分利和宏，前田達彦，増田寛之：ギャップブレースを取り付けた鉄骨架構の静的解析，日本建築学会大会学術講演梗概集，pp.953-954, 2020.9.

4) 高橋周吾，佐藤大樹，矢野将斗志，Alex Shegay，笠井和彦：ギャップブレースを有する鉄骨架構のブレース稼働に伴う影響その 3 実験結果と付加応力の評価，日本建築学会関東支部研究報告集，pp.289-292, 2022.3.

*1 東京工業大学 環境社会理工学院 大学院生
*2 東京工業大学 准教授·博士（工学）
*3 東京工業大学 名誉教授
*4 株式会社 竹中工務店
*5 東京工業大学 博士研究員

*1 Graduate Student, Tokyo Institute of Technology
*2 Associate Prof, Tokyo Institute of Technology, Dr. Eng.
*3 Honorary Prof., Tokyo Institute of Technology, Ph.D.
*4 Takenaka corporation
*5 Post PhD researcher, Tokyo Institute of Technology, PhD.